Available online at www.sciencedirect.com
SCIENCE DIRECT®
Biochemical and Biophysical Research Communications 338 (2005) 437–445
BBRC
www.elsevier.com/locate/ybbrc

Review

Thermophilic cytochrome P450 enzymes

Clinton R. Nishida, Paul R. Ortiz de Montellano *

Department of Pharmaceutical Chemistry, University of California, 600 16th Street, San Francisco, CA 94143-2280, USA

Received 30 June 2005
Available online 22 August 2005

Abstract

Thermophilic cytochrome P450 enzymes are of potential interest from structural, mechanistic, and biotechnological points of view. The structures and properties of two such enzymes, CYP119 and CYP175A1, have been investigated and provide the foundation for future work on thermophilic P450 enzymes.

Keywords: Thermophilic hemoprotein; P450 structure; P450 mechanism; P450 topological probes; Hyperbaric stability; Heme modification

The family of known thermophilic cytochrome P450 enzymes is small. Only three such enzymes have been obtained as pure proteins, all of which have been crystallized and had their structures determined. The first, and most extensively studied, of these three enzymes is CYP119 from *Sulfolobus solfataricus*. The gene for this P450 enzyme was first identified in the *S. solfataricus* genome by the group of Kennelly and co-workers [1]. Heterologous expression of the gene in *Escherichia coli* confirmed assignment of the encoded protein as the first thermophilic P450 enzyme [2,3]. A related P450 enzyme from *Sulfolobus tokodaii* sp. strain 7, named P450st, was later also cloned, expressed, and partially characterized [4]. The third thermophilic P450 enzyme for which structural information is available is CYP175A1 from *Thermus thermophilus* HB27 [5].

In addition to the three relatively well-characterized enzymes, evidence exists for the presence of thermophilic P450 proteins in other organisms. Thus, thermophilic progesterone hydroxylase activities have been reported for *Bacillus thermoglucosidasius* strain 12060 [6] and *Bacillus stearothermophilus* [7]. The genome of the latter organism has been partially sequenced and appears to encode a P450 enzyme, perhaps that responsible for the progesterone hydroxylase activity. A BLAST analysis of the currently available genomes of thermophilic organisms indicates the probable presence of two thermophilic P450 enzymes in *Picrophilus torridus* DSM9790 (PTO0085 and PTO1399). It is to be expected that as the genomes of further thermophilic organisms become available, additional thermophilic P450 enzymes will be discovered.

Thermophilic P450 enzymes are of potential interest from several points of view. Elucidation of the features that convey thermostability could lead to the modification of mesophilic proteins to convert them into more stable biocatalysts. The structural stability offered by thermophilic P450 enzymes can also be exploited to carry out mechanistic investigations that are difficult to perform with the mesophilic counterparts. Most importantly, thermophilic P450 enzymes have a rich potential utility as catalysts in industrial settings. In the following sections of this review, we summarize the information that is currently available on CYP119, P450st, and CYP175A1.

Crystal structures of CYP119

CYP119 from *S. solfataricus* has been heterologously expressed in *E. coli* and crystallized [8,9]. The crystal structure at a resolution of 1.93 Å [8] was first reported at approximately the same time as a homology model of the structure based on sequence alignment with five mesophilic templates: $P450_{cam}$, $P450_{BM-3}$, $P450_{eryF}$, $P450_{terp}$, and $P450_{nor}$ [10]. This first crystal structure of CYP119 was

* Corresponding author. Fax: +1 415 502 4728.
E-mail address: ortiz@cgl.ucsf.edu (P.R. Ortiz de Montellano).

0006-291X/$ - see front matter © 2005 Elsevier Inc. All rights reserved.
doi:10.1016/j.bbrc.2005.08.093

solved by molecular replacement using the structure of $P450_{eryF}$ as the template [8], but a structure of the same protein at a resolution of 1.5 Å was independently determined by multiple wavelength anomalous dispersion (MAD) [11]. Two years later, a 3.0 Å resolution structure of P450st from *S. tokodaii* strain 7 was reported [4]. P450st has a sequence identity of 64% with respect to CYP119 and is thus a closely related protein. The first two structures of CYP119 had either an imidazole or 4-phenylimidazole ligand coordinated to the heme iron atom [8], whereas the second set of structures had a water or 4-phenylimidazole as the distal iron ligand [11]. A structure of the water-coordinated Phe24Leu mutant of the enzyme was also reported [11]. Finally, the structure of the *S. tokadaii* P450st was obtained in a water-coordinated state [4].

CYP119, with a length of 368 residues versus the 414 residues of $P450_{cam}$ and 403 of $P450_{eryF}$, is significantly smaller than the known mesophilic P450 enzymes. The structure of CYP119 retains the typical P450-fold characteristic of all the crystallized P450 enzymes. The shorter length of CYP119 is largely accounted for by the fact that the protein lacks many of the N-terminal residues present in $P450_{cam}$ and $P450_{eryF}$. The other differences that contribute to the shorter length of CYP119 are distributed throughout the protein, particularly at surface turns [8]. As a result, CYP119 has a more compact structure than the other bacterial P450 enzymes.

As might be expected, the active site incorporates some of the most conserved regions of the protein. In particular, the cysteine ligand (Cys317) is situated within a region and in an environment that exhibits high conservation relative to those of other P450 enzymes [8]. On the distal side, the I-helix of the protein traverses the entire protein and provides a framework for assembly of the catalytic residues. These include not only the highly conserved Thr213, which facilitates activation of oxygen, but also additional threonine residues at positions 214 and 215. As in $P450_{BM-3}$, which also has a second threonine adjacent to the highly conserved threonine, Thr214 rather than Thr213 donates a hydrogen bond to the peptide oxygen of Gly210. The two molecules of CYP119 in the crystallographic asymmetric unit were bound through a zinc ion coordinated to Glu139 and His178 in each of the two protein molecules. However, this dimerization is likely to be an artifact of crystallization rather than a functional feature of the enzyme.

The most interesting feature of the active site revealed by a comparison of the crystal structures of the imidazole- and 4-phenylimidazole-coordinated proteins is a major rearrangement of the active site that allows it to snugly accommodate the two different ligands [8]. This structural rearrangement adjusts the dimensions of the active site so that they better complement the iron-bound ligand (Fig. 1). The F- and G-helices of the protein undergo the largest movements in the rearrangement, suffering a displacement of their backbone atoms of up to 6 Å. Thus,

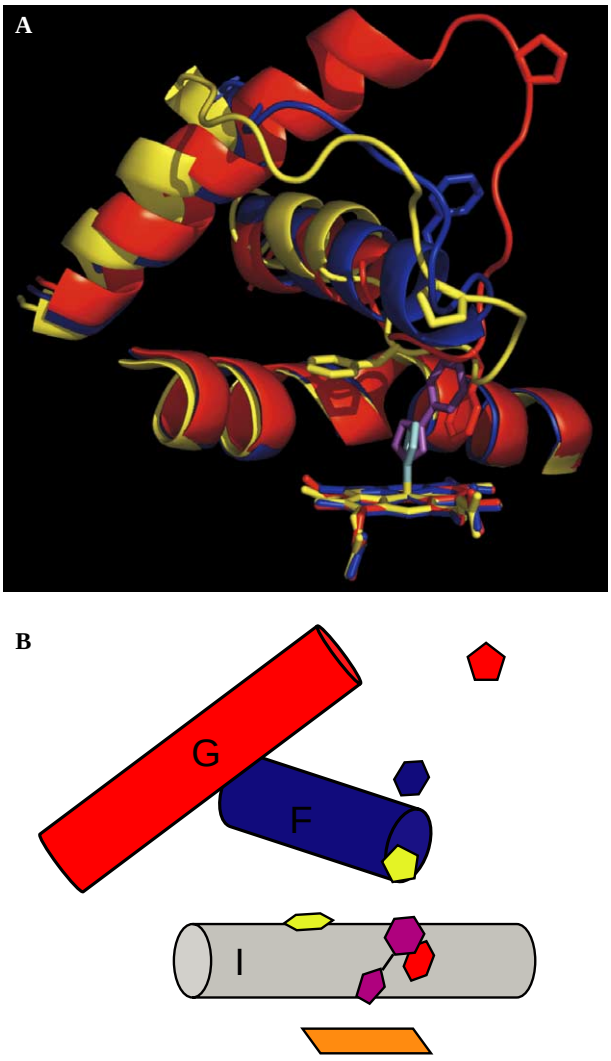

Fig. 1. (A) Structures of the active site of CYP119 in the ligand free state (red, PDB 1IO7), imidazole-bound state (yellow, PDB 1F4U, ligand in cyan), and 4-phenylimidazole-bound state (blue, PDB 1F4T, ligand in magenta), produced using PyMol software [39] following alignment of heme molecules using Deep View Swiss-PdbViewer software [40]. (B) Schematic representation of (A), highlighting the F/G loop structural difference between the ligand-free and imidazole-bound structures. Free pentagons represent Pro158, and free hexagons represent Phe153 side-chains. The longest representatives of the F (no ligand) and G (4-phenylimidazole-bound) helices are depicted in (B). Colors are the same as in (A). Most of the I-helix, which is relatively unchanged between the structures, is depicted in gray, and the heme groups in orange.

the F-helix in the 4-phenylimidazole complex is composed of residues 141–155, but in the imidazole complex the F-helix stops at residue 151 and thus encompasses four less residues. As a consequence, the F/G loop is lengthened and protrudes further into the active site, where it makes contacts with the imidazole ligand. This major conformational rearrangement displaces Arg154 from its position in the F-helix in the 4-phenylimidazole complex, where it hydrogen bonds to the peptidic oxygen of Glu198, to a position in the imidazole complex where it interacts with

Glu212. The loss of favorable interactions upon unraveling of the F-helix terminus is compensated for by new interactions between the F/G loop and the I-helix. The large conformational changes observed in the two CYP119 complexes are not unique, as large changes have also been observed in, for example, $P450_{BM-3}$ [12,13]. The large conformational shifts of CYP119 are nevertheless unusual. It is not yet known whether one or the other, or both, conformational states of CYP119 is catalytically active. The changes observed in these structures indicate that structural adjustment of the active site to complement specific substrates or ligands is possible and perhaps even not uncommon.

In the structure of CYP119 without an imidazole ligand [11], the iron binds a water molecule with an iron–oxygen distance of 2.27 Å. The water ligand is hydrogen-bonded to a second water at a distance of 2.93 Å. The distance from the thiolate sulfur to the iron on the proximal side is 2.27 Å. Although the overall structure is similar to that of imidazole-bound structures, the changes in the F/G loop area between the 4-phenylimidazole- and water-coordinated structures are even more dramatic than those between the 4-phenylimidazole- and imidazole-bound proteins [11]. The largest displacement of residues between the imidazole-bound and water-bound structures involves Pro158 and Gly159, which move distances of 13–18 Å. As a result, the F/G loop instead of dipping into the active site now extends outwards towards the surface of the protein (Fig. 1). The Phe153 side-chain in the ligand-free structure is part of the F/G loop and is positioned above (and directed toward) the heme. When the 4-phenylimidazole ligand binds, part of the F/G loop, including Phe153, becomes helical, extending the F-helix. As a result, the Phe153 side-chain flips up to the opposite side of the F-helix, away from the heme.

The hydrogen bonding network used to deliver protons for cleavage of the oxygen–oxygen bond, first noted in $P450_{cam}$ [14], is also present in CYP119. This network includes the acid group Glu212, Thr213, and two crystallographically defined water molecules [11].

The ferric protein, with a sharp Soret maximum at 415 nm and $\varepsilon = 104\ mM^{-1}$ [15,16], is in the low-spin state and undergoes only a small shift to the high-spin state as the temperature is raised [16]. Site-specific mutagenesis confirms that Thr213 is important for catalysis (vide infra) and shows that Thr214 helps to control the spin state [15]. Thus, upon mutation of Thr214 a higher (but still low, <20%) proportion of the protein is found in the high-spin state at both room temperature and 70 °C [15]. Mutation of Thr213 to larger residues (i.e., tryptophan) gives a protein that is to an even larger extent in the high-spin state but, as discussed below, has very low catalytic activity.

CYP119 active site structure probed by arylhydrazines

Cytochrome P450 enzymes have commonly been shown to react with aryldiazenes to give iron–aryl complexes. The aryldiazenes can be preformed or can be generated in situ from their arylhydrazine precursors. The resulting aryl–iron complexes are usually fairly stable, but oxidation of the protein complexes with ferricyanide triggers migration of the aryl group from the iron to one of the four porphyrin nitrogen atoms, giving an *N*-aryl heme derivative [17]. The direction of this iron-to-nitrogen shift is thought to be primarily controlled by steric clashes within the active site that channel the migration to the least sterically encumbered porphyrin nitrogen(s). The regioselectivity observed in the migration thus provides a rough topological map of the active site directly above the heme. This approach can be used to crudely map both the wild-type active site and the changes caused by either mutation of active site residues or conditions that perturb its structure.

The active site topology of CYP119 has been explored with a range of substituted aryldiazenes [18]. CYP119 reacts with a range of aryldiazenes to give the aryl–iron complexes, but it is exceptional in that the subsequent shift of the aryl group to give the *N*-aryl heme adducts occurs spontaneously under aerobic conditions without the addition of ferricyanide [18]. Oxygen is required for the shift, as it does not occur if the aryl–iron complexes are formed anaerobically. The rate of the aerobic aryl shift is decreased by electron-withdrawing substituents on the aryl ring, as shown by a Hammett ρ value of -1.50 determined from the rates of the shift reaction for a range of substituted aryldiazenes. Essentially the same electronic dependence ($\rho = -1.50$) is observed when the shift is promoted under anaerobic conditions by the addition of ferricyanide [18]. Interestingly, the shift does not seem to be very sensitive to the size of *p*-substituents, as approximately the same rate is observed for the phenyl-iron and *p*-biphenyl-iron shifts.

The aryl group in all of the *p*-substituted aryl–iron complexes preferentially shifts to the nitrogens of pyrrole rings C and D in wild-type CYP119 [18]. The isomer ratios range from $N_B{:}N_A{:}N_C{:}N_D = 00{:}00{:}29{:}71$ (*p*-CN) to 05:02:58:35 (4-CF_3). Only traces (0–5%) of the adducts of pyrrole rings A and B are observed. *Meta*-substituents appear to interfere with the shift, a finding that suggests a fairly high active site ceiling but the presence of steric congestion on the edges of the active site at small distances from the heme plane. The temperature dependence of the ratio of isomeric *N*-aryl heme adducts formed aerobically from the 4-nitrophenyl–iron complex indicated that temperature did not significantly modulate the topological interactions sensed by this probe, although at low temperatures the isomer ratio obtained anaerobically with ferricyanide differed by a small increment in the migration of the aryl group to pyrrole rings A and B [18]. At higher temperatures, both shift methods gave similar results. The aryl-shift data thus suggest that the active site is malleable but primarily open above pyrrole rings C and D.

The topological changes in the active site caused by mutations of Thr213 and Thr214 have been examined using the aryl-shift methodology [15]. The key probes employed were 4-trifluoromethylphenyldiazene (4-CF_3-C_6H_4-

N=NH) and 4-bromophenyldiazene (4-Br-C_6H_4-N=NH), both of which have electron-withdrawing substituents to slow down the shift reaction [15]. Whereas the wild-type enzyme gave an N_B:N_A:N_C:N_D ratio of 05:03:53:39 with the 4-trifluoromethylphenyl probe, the corresponding ratios for the T213A and T213S mutants were, respectively, 23:43:17:16 and 35:45:11:09. The corresponding ratios with the 4-bromophenyl probe were 05:03:55:36 for the wild-type, and 44:56:00:00 and 43:57:00:00 for the T213A and T213S mutants, respectively. The T213 mutants thus alter the active site so that the aryl group migrates exclusively to the pyrrole A and B rings rather than to the C and D rings favored in the wild-type protein. The T213V and T213W mutants gave approximately a wild-type pattern, as did the T214A and T214V mutants, indicating that in these mutants the gross active site topology was not greatly altered.

Thermal stability determinants

Based on the homology model [10] and the crystal structures of CYP119 [8,11], several factors have been proposed to contribute to its thermal stability: (a) a higher density of salt bridges, (b) a relatively low density of alanines coupled with a high incidence of isoleucines in the interior of the protein, resulting in better side-chain packing, and (c) the presence of extended aromatic clusters that are not present in mesophilic P450 structures. One aromatic cluster, which includes Tyr2, Trp4, Phe5, Phe24, Trp281, and Tyr15, spans an α-carbon-to-α-carbon distance of 11.3 Å. A second cluster that includes Phe225, Phe228, Trp231, Tyr250, Phe298, Phe334, and Phe338 spans a distance of ~24 Å between the α-carbons at the two termini (Fig. 2).

To test the hypothesis that the aromatic clusters contribute to thermal stability, several point mutants were expressed and purified: W231A, Y250A, W281A, Y2A/Y250A, W4A/W281A, and Y168A [19]. Studies of the thermal stability of the mutants compared to the wild-type enzyme using circular dichroism as the experimental parameter demonstrate that each of the resulting proteins has a melting point approximately 10 °C lower than that of the wild-type [19]. In an independent work, Maves and Sligar [16] carried out a random mutagenesis study of the stabilizing factors in CYP119 and demonstrated that the F24S mutant also suffered a loss of approximately 10 °C in thermal stability, although the F24L mutant only melted ~4 °C lower than the wild-type [11]. The structure of this mutant was determined and found to deviate in no obvious way from that of the wild-type other than in the volume occupied by the relevant side-chain [11]. Thus, disruption of the aromatic clusters by either a single or double mutation results in loss of approximately 10 °C in the stability of the protein.

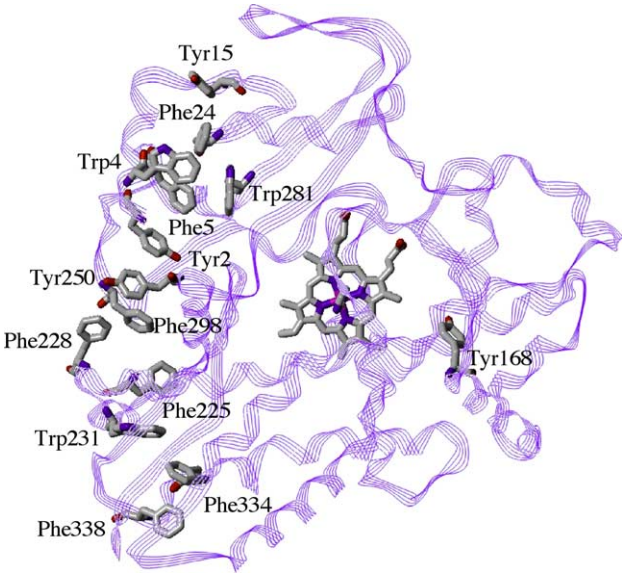

Fig. 2. Aromatic clusters on the surface of CYP119 that contribute to thermal stability of the protein.

The effect of other mutations on the thermal denaturation of CYP119 has also been examined. The difference in the active site conformation between the imidazole- and 4-phenylimidazole-bound proteins entails a critical change in the partnering of Arg154, a residue that connects the F–G helices. Arg154 hydrogen bonds with the peptide carbonyl of Glu163 in the phenylimidazole complex, but forms a salt bridge with Glu212 in the imidazole and water complexes. To determine whether this salt bridge contributes significantly to thermal stability, Glu212 was mutated to an aspartate or glutamine, and Arg154 was mutated to a glutamine or alanine [19]. However, the thermal stabilities of the mutant proteins were essentially the same as that of the wild-type, precluding an important role for these salt bridges in the thermal stability of the protein.

The possibility that the unusual triple threonine cluster in the I-helix might contribute to thermal stability, suggested by the finding that these residues help to keep the heme iron in the hexacoordinated state, has also been examined [15], but no decrease in the thermal stability of CYP119 was observed upon mutation of Thr213 and/or Thr214. In view of the fact that mutations of three I-helix residues located within the active site, Glu212, Thr213, and Thr214, do not alter thermal stability, it appears that the active site is structurally insulated and contributes little to the overall thermal stability of the protein.

In addition to the F24S mutation, eleven other mutations were found in the random mutagenesis study of Maves and Sligar [16] that caused some loss of thermal stability, although in some instances the decrease in melting point was only 2–3 °C. The largest changes in thermal stability were observed for the R295K (4.9 °C), S40C/T67A/V118L (4.3 °C), R235G/I282V/I299V/E352K (6.4 °C), and G313E (7.5 °C) mutations. Most of these residues are on the surface, but it is difficult to draw conclusions from these results, particularly from the multiple mutants that could simply introduce cumulative perturbations of the structure, other than to suggest that the results are consistent with a role for salt bridges in buttressing the structure.

Stability and structure of CYP119 under high pressure

The hyperbaric stability of CYP119 has also been investigated [20]. The mesophilic P450 enzymes so far studied denature irreversibly at high pressure. For example, $P450_{cam}$ is irreversibly inactivated at pressures above 130 MPa (1 MPa = 9.872 atm) [21]. In contrast, CYP119 was shown to withstand pressures up to 200 MPa without converting to the inactive P420 form [3]. Detailed studies have confirmed the pressure stability of CYP119, establishing that the pressure for half-inactivation of the protein (i.e., $P_{1/2}$ for conversion to the P420 form) was 380 MPa (20). Furthermore, these studies have led to a completely unexpected finding that in CYP119 denaturation to the P420 form is reversible [20]. Thus, upon decompression from 500 MPa, the enzyme rapidly and completely reverts to the active P450 state. The stability of the ferrous–CO complex was also examined. Only at a pressure of 400 MPa did the CO-bound protein begin to exhibit denaturation to the P420 form, but this denaturation was accompanied by precipitation and was not reversed by decompression [20]. A study of the temperature effect on inactivation by hyperbaric pressure established that protein denaturation increased at higher pressures as the temperature was increased, with a linear increase in the $P_{1/2}$ of 3.56 MPa/°C between 5 and 50 °C.

The pressure stability of the Thr213 and Thr214 mutants, in which the iron coordination and spin state are perturbed relative to the wild-type [15], was also examined [20]. Mutation of Thr213 to small residues that decreased the active site steric encumbrance had only small effects on the $P_{1/2}$ value, but mutation to Trp or Phe, which diminished the open active site volume, significantly stabilized the protein. Thus, at 20 °C, where the wild-type $P_{1/2}$ was 380 MPa, the $P_{1/2}$ of the T213F mutant was 550 MPa, and that of the T213W mutant 570 MPa [21]. Mutations of Thr214 to small residues had little effect on the pressure stability [21]. Regrettably, the thermal stability of the Thr213 mutants to large residues was not examined [15], nor the pressure stability of Thr214 mutations to residues with larger substituents.

A comparison of the active site topology under normal and hyperbaric conditions has been carried out using the iron–aryl shift technology already described [20]. Small increases in the proportions of the pyrrole ring A and B *N*-phenyl heme isomers were found at 400 MPa relative to the ratios obtained at normal pressure. When the same experiment was carried out with the T213A mutant, in which the aryl shift occurs mainly towards pyrrole rings A and B [15], a modest change favoring migration towards the other two (C and D) pyrrole ring nitrogens was observed at high pressure. When the pressure was released prior to promoting the shift with ferricyanide, the same results were obtained as were obtained with the unpressurized protein. Thus, the data indicate that the active site undergoes some degree of reversible deformation or contraction at high pressure.

Catalytic chemistry of CYP119

The endogenous substrates of CYP119 in *Sulfolobus solfataricus* and P450st in *Sulfolobus* sp. strain 7 are not known. An initial screen for potential substrates of CYP119 was carried out by searching for small compounds that could alter the spin state of the enzyme [15]. Only minor changes were observed with a range of such compounds, including styrene. Nevertheless, an NMR T_1 relaxation study established that styrene was bound within the active site of the enzyme with its protons within 4–7 Å of the heme iron atom. Resonance Raman data confirmed the low-spin state of the resting enzyme [15,22] and supported the conclusion that styrene causes a small shift in the spin state [15]. Styrene was therefore chosen as a potential first substrate with which to assay the catalytic activity of CYP119.

As the electron donor partners of CYP119 were not then known, the initial studies of styrene oxidation were carried out with H_2O_2 as a donor of oxidizing equivalents [15]. A clear conversion of styrene to styrene oxide was observed with a rate of 0.6 nmol min^{-1} $nmol^{-1}$ protein at 30 °C. Similar oxidation of *cis*- and *trans*-β-methylstyrenes to the corresponding epoxides occurred, as expected, with retention of configuration. A T213A mutation caused a decrease of 25% in the rate of styrene epoxidation, but much larger impairments of activity were observed when Thr213 was mutated to a valine, serine, phenylalanine, or tryptophan. In contrast, the T214A and T214V mutants exhibited a 3-fold enhancement of H_2O_2-dependent styrene epoxidation. Interestingly, styrene epoxidation by the T214A and T214V mutants could be supported by putidaredoxin and putidaredoxin reductase, albeit at a rate 100-fold lower than that obtained with H_2O_2 [15,23]. However, catalysis by the Thr213 mutants was not supported by this pair of surrogate electron donor proteins. These results suggest that the increased high-spin state obtained with the Thr214 mutants facilitates electron transfer, while mutations of Thr213, even if they increase the high-spin state, remove an important catalytic residue and suppress electron-dependent catalysis [15].

Fatty acids are better ligands for CYP119 than styrene [23]. The fatty acids give rise to a conventional Type I spectroscopic shift upon binding to the enzyme from which a binding affinity can be determined. Lauric acid binds with $K_s = 1.2$ μM, a value comparable to those obtained for the binding of myristic, palmitic, and stearic acids [23]. The 10-carbon capric acid binds somewhat less tightly ($K_s = 28$ μM), as does the 20-carbon arachidic acid ($K_s = 5$ μM). All these fatty acids binds much more tightly than styrene, which binds with $K_s = 530$ μM. The binding of lauric acid to the D77R, T214V, and D77R/T214V mutants showed that the T214V mutation decreases the K_s to 0.3–0.4 μM, in accord with the findings that the T214V mutation facilitated the spin state conversion and increased styrene binding [15]. The D77R mutation was introduced in the hope of improving the binding of putidaredoxin to

CYP119, and thus of increasing electron transfer and catalysis (vide infra) [23]. As this mutation is located outside the active site, it is not surprising that it has no effect on fatty acid binding.

Fatty acids are not only better ligands but also better substrates for CYP119. Using an optimized ratio of 1:20:1 CYP119:putidaredoxin:putidaredoxin reductase at 37 °C, lauric acid was oxidized to hydroxylauric acid with $K_m = 21\ \mu M$ and $V_{max} = 0.36\ min^{-1}$. The D77R mutation increased V_{max} to $4.71\ min^{-1}$, the T214V mutation to $2.08\ min^{-1}$, and the double mutation D77R/T214V to $8.80\ min^{-1}$. Analysis of the lauric acid oxidation products revealed that at room temperature ω-1 hydroxylation is favored (69–76%), followed by ω-2, ω-, and ω-3 hydroxylation (16–22%, 6–10%, and 1–4%, respectively), where the ranges encompass the findings for the wild-type, D77R, T214V, and D77R/T214V mutants.

Two other catalytic processes have been described for CYP119: (a) electrocatalytic reductive dehalogenation of CCl_4 to CH_4 [24], and (b) electrocatalytic reductions of nitrite, nitric oxide, and nitrous oxide [25]. Reversible electrochemical reduction of P450st under anaerobic conditions has also been demonstrated [4]. These reductive reactions are of interest from a biotechnological point of view, as similar reactions are known to be mediated by other P450 enzymes. In general, P450 reductive processes are much easier to support by electrochemical methods than oxidative processes because they circumvent the autooxidation and direct reduction of oxygen to peroxides that impair and/or terminate enzyme function.

Catalytic intermediates

The stability of CYP119 has led to efforts to employ this protein to characterize P450 catalytic species [22,26]. In a first study, Denisov et al. prepared the ferrous dioxygen complex of CYP119 at low temperature and characterized it by UV–Vis spectroscopy. The spectrum of the complex differed in subtle ways from that of the corresponding $P450_{cam}$ complex, but the source of the differences, which reflect differences in thiolate ligation of the heme iron and/or interactions of the dioxygen ligand with the protein environment, remain unclear. The dioxygen complex was shown to be unusually unstable towards autooxidation, decomposing at a rate of $\sim 0.08\ s^{-1}$ at 5 °C [22]. It is probable that the unusual properties of the active site deduced from the crystal structure contribute to this instability. These properties include: (a) a smaller displacement of the heme iron from the heme plane in the hexacoordinated state (0.09 Å out of the pyrrole nitrogen plane versus 0.30 Å for $P450_{cam}$), (b) a larger deviation of the Fe–S bond from the perpendicular to the heme plane in the substrate-free state (8.5° versus 2° in $P450_{cam}$), and (c) an unusually large ruffling of the porphyrin [22]. The higher stability of the low-spin state is also likely to contribute to rapid autooxidation of the oxyferrous complex.

Cryoreduction has been shown with $P450_{cam}$ to provide an elegant access to intermediates in the P450 catalytic cycle. In the $P450_{cam}$ studies, cryoreduction afforded the ferrous dioxy, ferric peroxo, and ferric hydroperoxo intermediates, although efforts to obtain the critical ferryl species by the same means gave equivocal results [27]. The same approach has been pursued with CYP119 [22]. Cryogenic radiolysis of the ferrous dioxy form of CYP119 yielded a species with a Soret maximum at 440 nm attributed, on the basis of its EPR spectrum and similarity to the corresponding species obtained with $P450_{cam}$, to the ferric peroxo complex. Annealing of this species gives rise to a two-step transformation above 160 K. The first step was thought to be protonation of the peroxo complex to give the low-spin ferric hydroperoxo complex, followed by dissociation of the peroxide to regenerate the ferric enzyme. No evidence was obtained for formation of the putative ferryl species.

In a second study, Kellner et al. [26] investigated the reaction of CYP119 with *meta*-chloroperbenzoic acid, a surrogate donor of activated oxygen. Rapid mixing of the enzyme with the peracid produced a species with absorption maxima at 370, 610, and 690 nm attributed to a ferryl porphyrin radical cation equivalent to that of a classical peroxidase Compound I. This intermediate formed at a rate of $3.20\ (\pm 0.3) \times 10^5\ M^{-1}\ s^{-1}$ at pH 7.0 at 4 °C and decomposed back to the ferric enzyme with a first-order rate constant of $29.4 \pm 3.4\ s^{-1}$. Adding lauric acid to the preformed intermediate resulted in quenching of the species within the dead time of the instrument and reportedly resulted in the formation of hydroxylauric acid, although the details of this experiment were not presented.

Other investigators have observed the formation of a ferryl-like species in the reactions of $P450_{cam}$ with peroxides [28–30]. The CYP119 experiments of Kellner et al. [26] represent an improvement over some of the earlier studies because the intermediate, although formed in low amounts, was more stable and therefore its formation and decay rates could be better determined. In the most recent study of the reaction of $P450_{cam}$ with a peracid, UV spectroscopic changes were interpreted in terms of initial formation of a peracid–iron complex, followed by formation of a ferryl/porphyrin radical cation and then a second species with a ferryl and a protein radical [30]. In the presence of peroxidase substrates, the protein was shown to have peroxidase activity. However, it is not yet clear that the species obtained with peroxides is the same as the catalytic species obtained under normal catalytic conditions. An intermediate with the same spectroscopic properties has not been observed in the cryogenic reduction experiments or any other oxygen-dependent process, and peroxidase activity is not observed under normal turnover conditions. It is to be noted that precedent exists for the formation of differentiable hemoprotein catalytic species with surrogate donors of electrons or activated oxygen. For example, heme oxygenase, which also employs electrons from cytochrome P450 reductase to activate

molecular oxygen, gives a distinguishable catalytic species when it is generated with electrons from ascorbate rather than cytochrome P450 reductase [31]. In another example, the turnover of cytochrome P450 enzymes by peroxides does not always give the same products as the P450-reductase-dependent turnover. A striking demonstration of this is the reported failure of hydrogen peroxide to support the ω-hydroxylation of fatty acids [32]. Thus, although promising, further work is required to link the species formed with *meta*-chloroperbenzoic acid with that formed under normal turnover conditions.

Electron donor partners

As already noted, earlier efforts to support the catalytic turnover of CYP119 with surrogate electron donor partners, notably putidaredoxin/putidaredoxin reductase or spinach ferredoxin/ferredoxin reductase, met with limited success [15]. Putidaredoxin and putidaredoxin reductase were at best inefficient electron donors for CYP119. Based on a comparison of the sequences and structures of CYP101 and CYP119, it was hypothesized that Asp77 in CYP119 was located in a possible binding site for putidaredoxin at a position where its negative charge would clash electrostatically with Asp34 in putidaredoxin, disfavoring binding of the electron donor protein [23]. The D77R mutant, which would convert the electrostatic interaction from a disfavorable to a favorable one, was therefore prepared. The D77R mutant was indeed found to accept electrons more efficiently from putidaredoxin than wild-type CYP119, although it is not yet clear if this improved function is due to the validity of the hypothesis that led to the mutation.

Measurements of the midpoint potential for CYP119 have established the value $E_m = -214 \pm 5$ mV for the wild-type and −227 mV for the D77R mutant [23]. These values are close to the value $E_m = -216$ mV for $P450_{cam}$. These results clearly show that inefficient reduction of CYP119 by putidaredoxin is not the consequence of an inaccessible reduction potential. Furthermore, they confirm that the D77R mutation does not accelerate reduction by altering the redox potential, providing some support for the postulated role of the electrostatic interaction in disfavoring (or favoring) the binding of putidaredoxin.

A search for potential redox partners for CYP119 in thermophilic organisms led to a screen of several thermophilic ferredoxins as potential partners. One of the systems examined was the ferredoxin from *S. tokodaii* strain 7, which had been reported by Wakagi and co-workers [33,34] in a non-P450 context. This ferredoxin has as its normal partner a 2-oxoacid:ferredoxin oxidoreductase rather than an NAD(P)H-dependent flavoprotein. To our delight, we found that this system efficiently reduces CYP119 and supports the oxidation of lauric acid [35]. This led us to clone out the corresponding ferredoxin and 2-oxoacid:ferredoxin oxidoreductase from *S. solfotaricus* [36]. Incubation of CYP119 with the two heterologously expressed proteins affords an efficient, high-temperature catalytic system. The maximum rate of lauric acid hydroxylation with this reconstituted system occurred at 70 °C, although good activity was retained during the course of a 20 min assay up to 90 °C. The enzyme system, however, lost some of its activity after incubation at 70 °C for 50 min, apparently as a result of a partial loss of activity of the 2-oxoacid:ferredoxin oxidoreductase. The pH optimum for the catalytic system was 4.5, in contrast to the pH optimum expected for the *S. tokodaii* strain 7 surrogate redox partners, as the 2-oxoacid:ferredoxin reductase from that organism has a pH optimum of 8.

P450st

The structure of P450st from *S. tokadaii* strain 7 has been determined but only to a resolution of 3 Å [4]. The structure of this substrate-free protein has a water coordinated to the heme iron atom. The r.m.s. deviations for the corresponding Cα atoms relative to the CYP119 (water coordinated) and CYP119 (imidazole-coordinated) structures are 1.2 and 1.4 Å, respectively. The structure is therefore very similar to that of CYP119, although the active site is poised in a conformational state between those observed for CYP119 with a distal water or imidazole ligand. This difference stems from the fact that the F-helix is slightly longer in P450st and that five additional residues have been inserted between the G and H helices. No other information is available on this protein.

CYP175A1

Relatively little is known about CYP175A1, the third thermophilic P450 enzyme for which structural information is available [5]. The enzyme is stable at 70 °C and has been reported to oxidize β-carotene to zeaxanthin [37]. The structure of the heterologously expressed enzyme has been determined to a resolution of 1.8 Å [5]. As with CYP119, the general P450 structure is conserved, but the large aromatic clusters found in CYP119 are not present in CYP175A1. The thermal stability of this enzyme is thus achieved through other mechanisms. Analysis of the protein structure has led to the proposal that the thermal stability of CYP175A1 derives from the unusual extent to which charged residues are assembled into salt-link networks rather than being present as single electrostatic pairs. As with CYP119, another factor that contributes to the thermal stability is the fact that the enzyme consists of only 389 residues, a number slightly larger than that of CYP119 (378 residues) but shorter than that, for example, of $P450_{cam}$ (414 residues) or the hemoprotein domain of $P450_{BM-3}$ (455 residues). Yano et al. [5] also argue that the protein contains fewer labile protein residues, among which they number asparagine, glutamine, and cysteine. Thus, although there are some common properties, comparison of the two thermophilic P450 structures confirms what is known from other thermophilic enzymes: i.e., that

nature has evolved multiple strategies for the thermal stabilization of proteins [38].

Acknowledgment

This work was supported by Grant GM25515 from the National Institutes of Health.

References

[1] R.L. Wright, K. Harris, B. Solow, R.H. White, P.J. Kennelly, Cloning of a potential cytochrome P450 from the archaeon *Sulfolobus solfataricus*, FEBS Lett. 384 (1996) 235–239.
[2] L.S. Koo, P.R. Ortiz de Montellano, Heterologous expression and characterization of CYP119 from the archaeon, *Sulfolobus solfataricus*, FASEB J. 9 (1997) A813.
[3] M.A. McLean, S.A. Maves, K.E. Weiss, S. Krepich, S.G. Sligar, Characterization of a cytochrome P450 from the acidothermophilic archaea *Sulfolobus solfataricus*, Biochem. Biophys. Res. Commun. 252 (1998) 166–172.
[4] Y. Oku, A. Ohtaki, S. Kamitori, N. Nakamura, M. Yohda, H. Ohno, Y. Kawarabayashi, Structure and direct electrochemistry of cytochrome P450 from the thermoacidophilic crenarchaeon, *Sulfolobus tokodaii* strain 7, J. Inorg. Biochem. 98 (2004) 1194–1199.
[5] J.K. Yano, F. Blasco, H. Li, R.D. Schmid, A. Henne, T.L. Poulos, Preliminary characterization and crystal structure of a thermostable cytochrome P450 from *Thermus thermophilus*, J. Biol. Chem. 278 (2003) 608–616.
[6] O. Sideso, R.A.D. Williams, S.G. Welch, K.E. Smith, Progesterone 6-hydroxylation is catalysed by cytochrome P450 in the moderate thermophile *Bacillus thermoglucosidasius* strain 12060, J. Steroid. Biochem. Mol. Biol. 67 (1998) 163–169.
[7] S. Al-Awadi, M. Afzal, S. Oommen, Studies on *Bacillus stearothermophilus*. Part III. Transformation of testosterone, Appl. Microbiol. Biotech. 62 (2003) 48–52.
[8] J.K. Yano, L.S. Koo, D.J. Schuller, H. Li, P.R. Ortiz de Montellano, T.L. Poulos, Crystal structure of a thermophilic cytochrome P450 from the archaeon *Sulfolobus solfataricus*, J. Biol. Chem. 275 (2000) 31086–31092.
[9] S.Y. Park, K. Yamane, S. Adachi, Y. Shiro, K.E. Weiss, S.G. Sligar, Crystallization and preliminary X-ray diffraction analysis of a cytochrome P450 (CYP119) from *Sulfolobus solfataricus*, Acta Crystallogr. D 56 (2000) 1173–1175.
[10] Y.T. Chang, G.H. Loew, Homology modeling, molecular dynamics simulations, and analysis of CYP119, a P450 enzyme from extreme acidothermophilic archaeon *Sulfolobus solfataricus*, Biochemistry 39 (2000) 2484–2498.
[11] S.-Y. Park, K. Yamane, S. Adachi, Y. Shiro, K.E. Weiss, S.A. Maves, S.G. Sligar, Thermophilic cytochrome P450 (CYP119) from *Sulfolobus solfataricus*: high resolution structure and functional properties, J. Inorg. Biochem. 91 (2002) 491–501.
[12] H. Li, T.L. Poulos, The structure of the cytochrome P450BM-3 haem domain complexed with the fatty acid substrate, palmitoleic acid, Nat. Struct. Biol. 4 (1997) 140–146.
[13] Y.-T. Chang, G.H. Loew, Molecular dynamics simulations of P450 BM3—examination of substrate-induced conformational change, J. Biomol. Struct. Dyn. 16 (1999) 1189–1203.
[14] T.M. Makris, I. Denisov, I. Schlichting, S.G. Sligar, Activation of molecular oxygen by cytochrome P450, in: P.R. Ortiz de Montellano (Ed.), Cytochrome P450: Structure, Mechanism, and Biochemistry, third ed., Kluwer Academic/Plenum, New York, 2005, pp. 149–182.
[15] L.S. Koo, R.A. Tschirret-Guth, W.E Straub, P. Moënne-Loccoz, T.M. Loehr, P.R. Ortiz de Montellano, The active site of the thermophilic CYP119 from *Sulfolobus solfataricus*, J. Biol. Chem. 275 (2000) 14112–14123.
[16] S.A. Maves, S.G. Sligar, Understanding thermostability in cytochrome P450 by combinatorial mutagenesis, Protein Sci. 10 (2001) 161–168.
[17] P.R. Ortiz de Montellano, Arylhydrazines as probes of hemoprotein structure and function, Biochimie 77 (1995) 581–593.
[18] R.A. Tschirret-Guth, L.S. Koo, P.R. Ortiz de Montellano, Protein control of the formation and decomposition of CYP119 and CYP101 aryl-iron complexes, J. Biol. Inorg. Chem. 5 (2000) 204–212.
[19] A.V. Puchkaev, L.S. Koo, P.R. Ortiz de Montellano, Aromatic stacking as a determinant of the thermal stability of CYP119 from *Sulfolobus solfataricus*, Arch. Biochem. Biophys. 409 (2003) 52–58.
[20] R.A. Tschirret-Guth, L.S. Koo, G. Hui Bon Hoa, P.R. Ortiz de Montellano, Reversible pressure deformation of a thermophilic cytochrome P450 enzyme (CYP119) and its active-site mutants, J. Am. Chem. Soc. 123 (2001) 3412–3417.
[21] G. Hui Bon Hoa, C. Di Primo, I. Dondaine, S.G. Sligar, I.C. Gunsalus, P. Douzou, Conformational changes of cytochrome P450cam and P450lin induced by high pressure, Biochemistry 28 (1989) 651–656.
[22] I.G. Denisov, S.C. Hung, K.E. Weiss, M.A. McLean, Y. Shiro, S.Y. Park, P.M. Champion, S.G. Sligar, Characterization of the oxygenated intermediate of the thermophilic cytochrome P450 CYP119, J. Inorg. Biochem. 87 (2001) 215–226.
[23] L.S. Koo, C.E. Immoos, M.S. Cohen, P.J. Farmer, P.R. Ortiz de Montellano, Enhanced electron transfer and lauric acid hydroxylation by site-directed mutagenesis of CYP119, J. Am. Chem. Soc. 124 (2002) 5684–5691.
[24] E. Blair, J. Greaves, P.J. Farmer, High-temperature electrocatalysis using thermophilic P450 CYP119: dehalogenation of CCl_4 to CH_4, J. Am. Chem. Soc. 126 (2004) 8632–8633.
[25] C.E. Immoos, J. Chou, M. Bayachou, E. Blair, J. Greaves, P.J. Farmer, Electrocatalytic reductions of nitrite, nitric oxide, and nitrous oxide by thermophilic P450 CYP119 in film-modified electrodes and an analytical comparison of its catalytic activities with myoglobin, J. Am. Chem. Soc. 126 (2004) 4934–4942.
[26] D.G. Kellner, S.C. Hung, K.E. Weiss, S.G. Sligar, Kinetic characterization of compound I formation in the thermostable cytochrome P450 CYP119, J. Biol. Chem. 277 (2002) 9641–9644.
[27] I. Schlichting, J. Berendzen, K. Chu, A.M. Stock, S.A. Maves, D.E. Benson, R.M. Sweet, D. Ringe, G.A. Petsko, S.G. Sligar, The catalytic pathway of cytochrome P450cam at atomic resolution, Science 287 (2000) 1615–1622.
[28] V. Schünemann, C. Jung, A.X. Trautwein, D. Mandon, R. Weiss, Intermediates in the reaction of substrate-free cytochrome P450cam with peroxy acetic acid, FEBS Lett. 479 (2000) 149–154.
[29] T. Egawa, H. Shimada, Y. Ishimura, Evidence for Compound I formation in the reaction of cytochrome P450cam with m-chloroperbenzoic acid, Biochem. Biophys. Res. Commun. 201 (1994) 1464–1469.
[30] T. Spolitak, J.H. Dawson, D.P. Ballou, Reaction of ferric cytochrome P450cam with peracids. Kinetic characterization of intermediates on the reaction pathway, J. Biol. Chem. 280 (2005) 20300–20309.
[31] J. Wang, L. Lad, T.L. Poulos, P.R. Ortiz de Montellano, Regiospecificity determinants of human heme oxygenase. Differential NADPH- and ascorbate-dependent heme cleavage by the R183E mutant, J. Biol. Chem. 280 (2005) 2797–2806.
[32] A. Ellin, S. Orrenius, Hydroperoxide-supported cytochrome P450-linked fatty acid hydroxylation of liver microsomes, FEBS Lett. 50 (1975) 378–381.
[33] E. Fukuda, H. Kino, H. Matsuzawa, T. Wakagi, Role of a highly conserved YPITP motif in 2-oxoacid:ferredoxin oxidoreductase. Heterologous expression of the gene from *Sulfolobus* sp. strain 7, and characterization of the recombinant and variant enzymes, Eur. J. Biochem. 268 (2001) 5639–5646.
[34] K. Kojoh, H. Matsuzawa, T. Wakagi, Zinc and an N-terminal extra stretch of the ferredoxin from a thermoacidophilic archaeon stabilize the molecule at high temperature, Eur. J. Biochem. 264 (1999) 85–91.

[35] A.V. Puchkaev, T. Wakagi, P.R. Ortiz de Montellano, CYP119 plus a *Sulfolobus tokodaii* strain 7 ferredoxin and 2-oxoacid:ferredoxin oxidoreductase constitute a high temperature cytochrome P450 catalytic system, J. Am. Chem. Soc. 124 (2002) 12682–12683.

[36] A.V. Puchkaev, P.R. Ortiz de Montellano, The *Sulfolobus solfataricus* electron donor partners of thermophilic CYP119. An unusual non-NAD(P)H-dependent cytochrome P450 system, Arch. Biochem. Biophys. 434 (2005) 169–177.

[37] F. Blasco, I. Kauffman, R.D. Schmid, CYP175A1 from *Thermus thermophilus* HB27, the first beta-carotene hydroxylase of the P450 superfamily, Appl. Microbiol. Biotechnol. 64 (2004) 671–674.

[38] A. Szilgyi, P. Závodszky, Structural differences between mesophilic, moderately thermophilic and extremely thermophilic protein subunits: results of a comprehensive survey, Structure 8 (2000) 493–504.

[39] W.L. DeLano, The PyMOL Molecular Graphics System, DeLano Scientific, San Carlos, CA, USA, 2002. <http://www.pymol.org>.

[40] N. Guex, M.C. Peitsch, SWISS-MODEL and the Swiss-Pdb-Viewer: An environment for comparative protein modeling, Electrophoresis 18 (1997) 2714–2723. <http://www.expasy.org/spdbv/>.